nature communications

Article

https://doi.org/10.1038/s41467-024-54907-6

Human interventions have enhanced the net ecosystem productivity of farmland in China

Received: 28 January 2024

Accepted: 25 November 2024

Published online: 03 December 2024

Check for updates

Sun Zhang[1], Wei Chen[1] ✉, Yanan Wang[1] ✉, Qiao Li[1], Haimeng Shi[1], Meng Li[1], Zhongxiao Sun[2], Bingrui Zhu[1] & Gezahegne Seyoum[1]

Human interventions, such as farmland management, have long been considered crucial for soil carbon sequestration, but little is known about the exact impact of these interventions on the net carbon flux, represented by net ecosystem productivity (NEP). Here, using multiple long-term, large-scale data and statistical data, we reveal that 75.54% of farmland NEP in China experiences an increase, with northern regions showing the greatest potential for future farmland carbon sequestration. This growth is primarily attributed to the role of farmland management, especially the enhancement of no-tillage, land consolidation and multiple cropping level (17.02%, major grain-producing areas in 2020). Notably, the current unreasonable practices of mechanized straw returning and irrigation have a negative impact on farmland NEP. Our results show that it is imperative to acknowledge the crucial role of human interventions on farmland NEP to strike a balance between food security and farmland carbon sequestration.

Terrestrial ecosystems serve as vital carbon sinks, absorbing approximately one-third of annual carbon emissions[1,2], and have wielded significant influence over the global carbon cycle[3,4]. Farmland (12% of the Earth's ice-free land surface[5]), an ecosystem that accounts for nearly a third of terrestrial net primary productivity (NPP)[6], and is the primary source of sustenance for humanity, providing food, feed, and fuel[7,8], is particularly susceptible to human impacts. Similar to climate change, farmland management practices have long been considered to exert control on carbon sequestration in farmland ecosystems[9–12]. Understanding how the net uptake of carbon dioxide by farmland ecosystem (denoted here by net ecosystem productivity, NEP) responds to human interventions is an important ecological issue.

The farmland ecosystem is among the most externally influenced terrestrial ecosystems[6,13], facing the dual challenges of climate change and human interventions such as farmland management[14,15]. The intensification of extreme weather events has significantly reduced terrestrial primary productivity, adversely affected terrestrial carbon sinks and increased pressure on global food security[1,16,17]. Additionally, human interventions can affect the supply of crop residues, grain yields, and soil carbon inputs[10,18,19], promoting the soil carbon sequestration of farmland[9]. Appropriate fertilization and irrigation can promote plant growth and increase soil carbon input[9,12]. Meanwhile, the adoption of the no-tillage (NT) system can alter the physical and chemical structure of the soil, enhancing carbon accumulation[20,21]. However, continuous mechanized straw returning (MSR) leads to a certain level of residual straw components in the soil, which limits further straw degradation and hinders soil carbon sequestration[22]. Mounting evidence suggests that farmland management practices can enhance soil carbon input[9], capture atmospheric carbon[20,23], reduce greenhouse gas emissions, and ensure food security[24,25]. Although the impacts of various human interventions on soil carbon storage have been studied, their effects on ecosystem carbon dynamics have rarely been investigated.

As the largest developing country and the highest emitter of greenhouse gases[2], China has managed to feed nearly 20% of the world's population with less than 10% of the world's farmland, leading to enormous pressures in terms of food security and carbon emission reduction[5]. Due to the spatial mismatch between grain production and consumption capacities in China[26], the Chinese government has designated major grain-producing areas (MGPA), major grain sales areas (MGSA) and production and sales balance areas (PSBA) to optimize grain production layout and ensure food security[27]

[1]College of Economics and Management, Northwest A&F University, Yangling, China. [2]College of Land Science and Technology, China Agricultural University, Beijing, China. ✉e-mail: chen_wei@nwafu.edu.cn; wyn3615@nwafu.edu.cn

(Supplementary Fig. 2). The MGPA accounts for 64% of China's farmland and nearly 75% of grain output[28] and is a potential area for farmland carbon sequestration. The grain production and consumption of PSBA are roughly balanced, while the MGSA has a high grain demand but insufficient production capacity. China's grain production regions differ significantly in terms of farmland area, yield, regional economic development, and natural conditions, leading to varying intensities of human interventions. Consequently, the division of these three grain production regions provides a unique opportunity to explore the impact of human interventions on farmland NEP, which cannot be achieved by traditional geographical divisions. The MGPA is the core region of agricultural production in China and the key implementation area of agricultural policies[28]. It is characterized by intensive agricultural production activities and has been subject to a high intensity of human interventions, which has greatly affected ecological processes in, for example, the soil environment[29,30]. Along with ensuring food production, the region also shoulders the task of reducing carbon emissions and enhancing carbon sequestration[28]. Thus, focusing on the impact of human interventions on farmland NEP in the MGPA can provide a scientific foundation for enhancing the carbon sequestration capacity of farmland, while also balancing food production and ecological conservation.

NEP typically reflects the dynamic carbon sequestration capacity of photosynthesis and respiration within ecosystems. China's NEP has been steadily increasing[31], but the spatiotemporal changes in farmland NEP in China are still uncertain. In addition, much less is known about the impact of human interventions on farmland NEP, which restricts our understanding of the carbon balance in farmland ecosystem, and no systematic mechanism has yet been proposed to explain the responses to human interventions. Therefore, understanding whether and to what extent various farmland management practices can have a beneficial impact on farmland NEP is crucial for determining the possible contribution of future farming systems to the mitigation of climate change.

In this study, we investigate the historical trajectories and influencing factors of farmland NEP in China by analyzing NEP data and land-use/land-cover change dataset, as well as human intervention data. Four farmland NEP datasets have been generated, with the first dataset serving as the baseline and the other three datasets being calibrated ("Methods", Supplementary Fig. 1). Here we detect temporal and spatial scale changes in farmland NEP (Fig. 1a), and examine the factors contributing to the increase in farmland NEP and its response to climate and various human interventions. Subsequently, we focus on evaluating the mechanisms of human interventions on carbon sequestration in the MGPA and analyzing the various processes of the carbon cycle. The purpose of this study is to explore the relationship between human interventions and farmland NEP—taking China as an example—and to depict the process of carbon cycling.

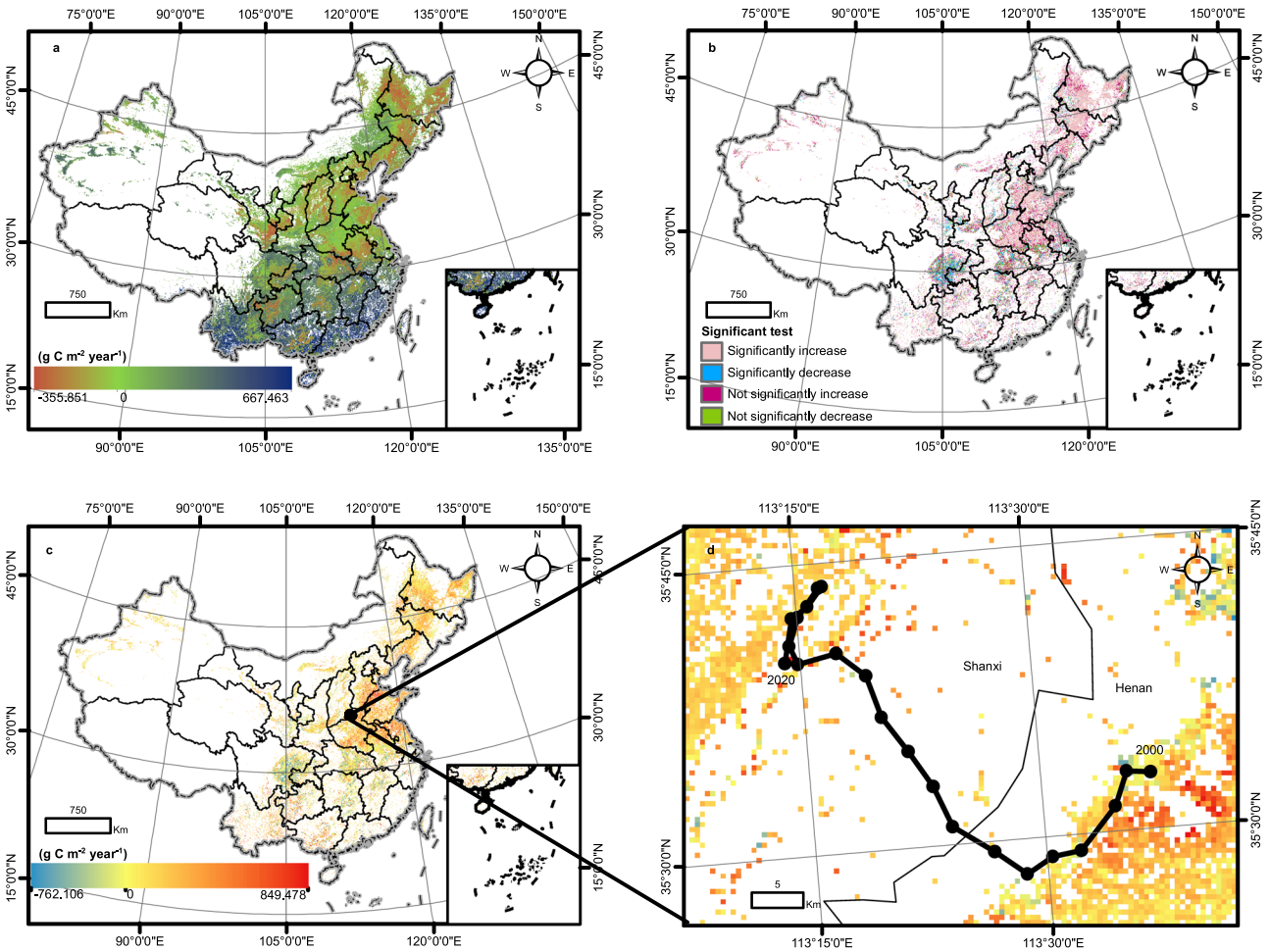

Fig. 1 | Spatial distribution of farmland NEP in China from 2000 to 2020. a The average annual distribution of China's farmland NEP from 2000 to 2020. The spatial patterns for specific years are shown in Supplementary Fig. 1. **b** Significant test of farmland NEP trend changes. **c** The difference in farmland NEP from 2000 to 2020. **d** Enlarged view showing the changing location of the center of gravity of farmland NEP. The variation in the position of the center of gravity of the calibrated farmland NEP is depicted in Supplementary Fig. 8. The base map was obtained from the standard map service of the Ministry of Natural Resources of the People's Republic of China. NEP net ecosystem productivity.

https://doi.org/10.1038/s41467-024-54907-6

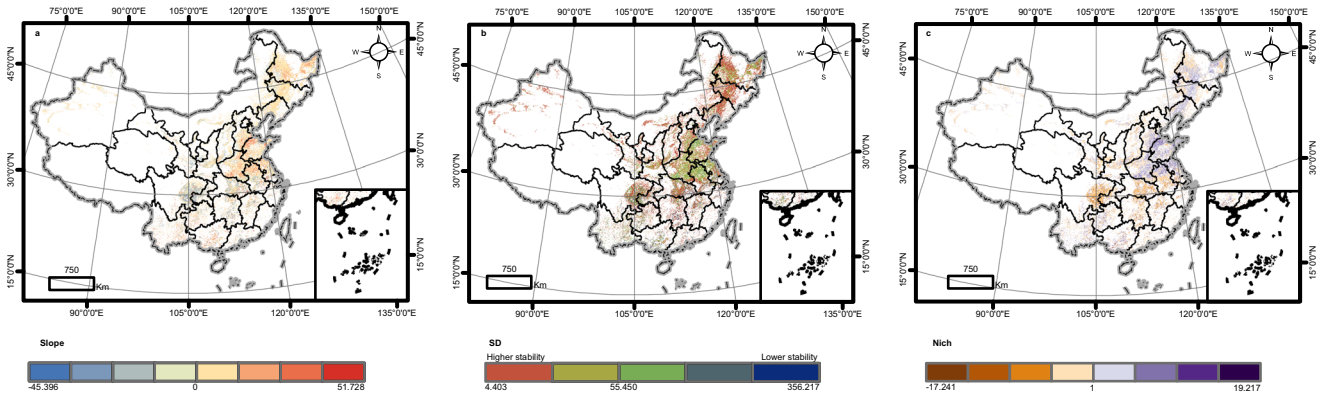

Fig. 2 | The spatial characteristics of farmland NEP in China from 2000 to 2020. **a** Trend changes of farmland NEP. The trend changes in farmland NEP were assessed through a unary linear regression method. A positive slope indicates an increasing trend in farmland NEP over the study period, whereas a negative slope indicates a decreasing trend. **b** The stability of farmland NEP. The standard deviation (SD) is used to indicate the stability of farmland NEP. A larger SD value signifies greater interannual variation of farmland NEP during the study period, reflecting lower stability. **c** The difference between the changes in farmland NEP in each grid and the overall changes from 2000 to 2020. The relative development rate (NICH) reflects changes in relative growth. A NICH value greater than 1 signifies that the growth rate of farmland NEP within the grid exceeds the overall development rate, while a value less than 1 indicates a growth rate lower than the overall development rate. The base map was obtained from the standard map service of the Ministry of Natural Resources of the People's Republic of China. NEP net ecosystem productivity.

Results and discussion

Historical changes of farmland NEP

To analyze the changes in farmland NEP, we use farmland and NEP data for China from 2000 to 2020 ("Methods"). The results indicate that the farmland NEP values in 33 province-level administrative units consistently increased over this period, with the highest values occurring in the southern region (such as Hainan 245.43 g C $m^{-2}year^{-1}$ and Fujian 211.26 g C $m^{-2}year^{-1}$) (Supplementary Fig. 1). Considering the uncertainty in the temporal trend of this farmland NEP, we used three other sets of calibration data ("Methods", Supplementary Fig. 3), which yielded similar results. Substantial changes have also taken place in the southern regions (Supplementary Fig. 4), exemplified by Guangxi's noteworthy increase of 80.29 g C $m^{-2}year^{-1}$ from 2000 to 2020 (from 38.82 g C m^{-2} $year^{-1}$ in 2000 to 119.11 g C m^{-2} $year^{-1}$ in 2020). Notably, the major grain-producing provinces in the northern regions have also experienced significant increases (Supplementary Fig. 1), with an increase from −80.32 g C $m^{-2}year^{-1}$ in 2000 to −21.82 g C $m^{-2}year^{-1}$ in 2020, representing a rise of 58.50 g C $m^{-2}year^{-1}$. From 2000 to 2020, China's farmland NEP has increased by 48.15 g C $m^{-2}year^{-1}$, with a particularly notable increase around 2010, when there was a peak in carbon sequestration capacity.

The growth rate of farmland NEP was relatively fast during the first 11 years of the study period but weakened in the subsequent 10-year periods. The initial significant increase in farmland NEP during the first decade of the 21st century can be ascribed to the interruption of climate warming causing a slowdown in ecosystem respiration and stimulation of gross primary productivity in the Northern Hemisphere[32–34] (Supplementary Fig. 5). Furthermore, the center of gravity of China's farmland NEP has shifted northwestward by 44.94 km, transitioning from 113.62°E, 35.55°N in 2000 to 113.23°E, 35.67°N in 2020 (Fig. 1c, d). This shift indicates that the rate of increase of farmland carbon sequestration capacity in the southeast has been slower than in the north (an increase of 27.37 g C $m^{-2}year^{-1}$ in the southeast, an increase of 41.51 g C $m^{-2}year^{-1}$ in the northwest). Typically, crops with deeper and larger root systems exhibit a greater carbon sequestration capacity[35]. Among cereal crops, wheat and corn are now predominantly cultivated in the northern regions, with increased planting yields (Supplementary Fig. 6). Their roots are larger and deeper than those of other crops, such as rice[36], which increases the carbon sequestration rate. Against the background of grain transportation from north to the south, there is a trend of farmland shifting northward, accompanied by a decline in the sowing area of grains in the southern regions, while witnessing an increase in the western and northern regions (Supplementary Fig. 7). This shift in the sowing area of grains further facilitates the migration of the center of gravity of farmland NEP towards the northwest direction.

Taking 2010 as the boundary, China's farmland has shifted from a carbon source area to a carbon sink area. It is noteworthy that 75.54% of China's farmland is now displaying an increasing trend in carbon sequestration capacity, which corresponds to the expansion of the farmland carbon sink area from 0.719 million km^2 to 0.931 million km^2 (an increase from 38.70 to 51.66%) (Supplementary Fig. 9). The trend is particularly apparent in most parts of northern China, where an annual increase of approximately 2.29 g C m^{-2} is observed (Fig. 2a). This is associated with farmland management in the region, including measures such as fertilization, which improves soil structure, enhances water and fertilizer, and stimulates plant root production[12], leading to enhanced plant production and carbon sequestration[18].

A significance analysis demonstrates that 51.48% of farmland NEP has increased significantly, with the northern region contributing 69.21% of this increase (30.79% in the southern) (Fig. 1b and Supplementary Fig. 10). The carbon sequestration capacity of farmland has been enhanced, with a significant increase in carbon sink area in the northern region, rising significantly from 28.90 to 47.67% (in the southern region, from 52.16 to 57.11%) (Supplementary Fig. 10b, c). The stability of farmland NEP is reflected by the standard deviation, with larger values indicating more variation in the farmland NEP data. Notably, 18.15% of China's farmland falls within the low stability range (Fig. 2b). This low stability is primarily observed in the North China Plain, although it also occurs to a certain extent in the Sichuan region in the Southwest. The increase in farmland NEP in areas with low stability is significantly greater than the overall increase in China as a whole (Fig. 2c). This distribution pattern aligns with the observed trends in farmland NEP, where regions with larger trends tend to have lower stability, predominantly concentrated in the MGPA of the northern region. Changes in grain yields and grain sowing areas (Supplementary Figs. 6 and 7), coupled with the active adoption of various farmland management practices, have increased the carbon sequestration capacity in these regions, consequently leading to lower stability.

Given the continuous increase of farmland NEP, highlights the important role of Chinese farmland in carbon sequestration[37], the

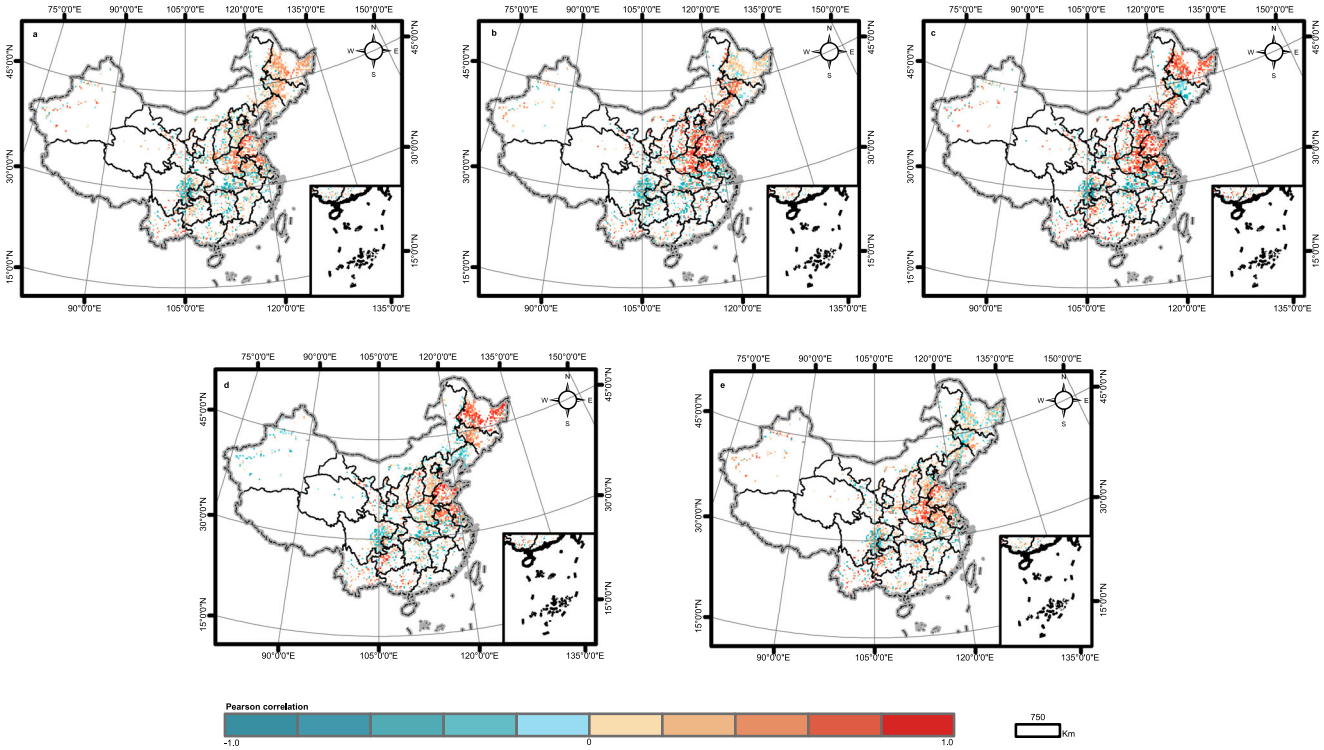

Fig. 3 | Correlations between farmland NEP and major human interventions in China from 2000 to 2020. a Land consolidation (LC); **b** no-tillage (NT); **c** mechanized straw returning (MSR); **d** irrigation degree per unit area (ID); **e** multiple cropping level (MC). The correlation coefficient (R) ranges from −1 to 1, with values greater than 0 indicating a positive correlation and values less than 0 indicating a negative correlation. The base map was obtained from the standard map service of the Ministry of Natural Resources of the People's Republic of China. NEP net ecosystem productivity.

reasons behind its spatial distribution characteristics are also interesting. The distribution of farmland NEP is influenced by water and heat conditions[13], the water and heat conditions in the southern region are significantly better than those in the northern region, resulting in significantly higher values of farmland NEP (Fig. 1). Notably, the northern region has had a significantly faster growth rate than the southern region: a phenomenon likely related to increased production of wheat and corn in the northern since the beginning of the 21st century (Supplementary Fig. 6). As wheat and corn are among the most efficient crops for carbon sequestration[35,36], their substantial yield increases have resulted in a faster growth rate in northern farmlands compared to the southern regions. Among them, the wheat production in the northern region increases from 72.085 Mt to 96.053 Mt, while in the southern region it increases from 27.551 Mt to 38.201 Mt. The corn production in the northern increases from 79.329 Mt to 216.921 Mt, and in the southern region it increases from 26.671 Mt to 43.745 Mt.

Furthermore, it may also be related to the increase in precipitation in the northern region in the early 21st century due to the northward movement of rain bands associated with the East Asian summer monsoon (Supplementary Fig. 5)[34]. The farmland NEP in the northeast region has a strong correlation with precipitation (Supplementary Fig. 11a), which plays a crucial role in plant photosynthesis[34,38]. The carbon sequestration effect of farmland in the south is stronger than that in the north: an effect that is associated with land use change. The inclusion of land such as mudflats and mixed agricultural-fruit areas in farmland is a cause of some uncertainty factors. The southern region has significantly more of these types of land compared to the northern region, and this difference will affect the biomass and carbon storage capacity of farmland areas[39]. Non-grain crops are common in the south and will lead to an increased biomass carbon storage. Additionally, the southern regions benefit from better photothermal conditions, allowing for multiple crop cycles within a single year. Diversified crop rotation can increase crop yield and reduce greenhouse gas emissions[25].

Attribution of changes in farmland NEP to human interventions

Next, we investigated the relevant relationship between human interventions and farmland NEP from the perspective of a national pattern ("Methods"). In the MGPA, the interannual variation of farmland NEP is positively correlated with major human intervention activities, especially in the warm monsoon areas (Fig. 3). The northeast region is the commodity grain base of China[40], and has its focus on the cultivation of rice and corn, resulting in a gradual decrease in the dedicated planting area for wheat and vegetables in the region. At high latitudes and under arid conditions, the wheat planting proportion (WP) and the vegetable planting proportion (VP) are negatively correlated with farmland NEP (Supplementary Fig. 11f, j), further confirming that in these areas, neither WP nor VP increases carbon sequestration. The concentration of precipitation in the summer, the prolonged winter, and the permafrost soil[41] make the large-scale cultivation of wheat and vegetable impractical. This shift reaffirms that the corresponding increase in the total value of farmland NEP is minimally impacted by planting structure and can be predominantly attributed to human interventions, particularly farmland management practices such as land consolidation (LC) and multiple cropping level (MC).

In light of this result, we examined the response of farmland NEP to various human intervention factors ("Methods") and found that farmland NEP is highly sensitive to changes in MC. At 0.277, the absolute values of sensitivity coefficients for NT are among the highest of any of the factors. Conversely, VP (−0.003) exhibits the smallest sensitivity (Fig. 4a). In the first period (before 2009), the sensitivity coefficient decreased year by year (excluding WP), while in the second period (2010–2020) the trend assumes a right leaning "V" shape

https://doi.org/10.1038/s41467-024-54907-6

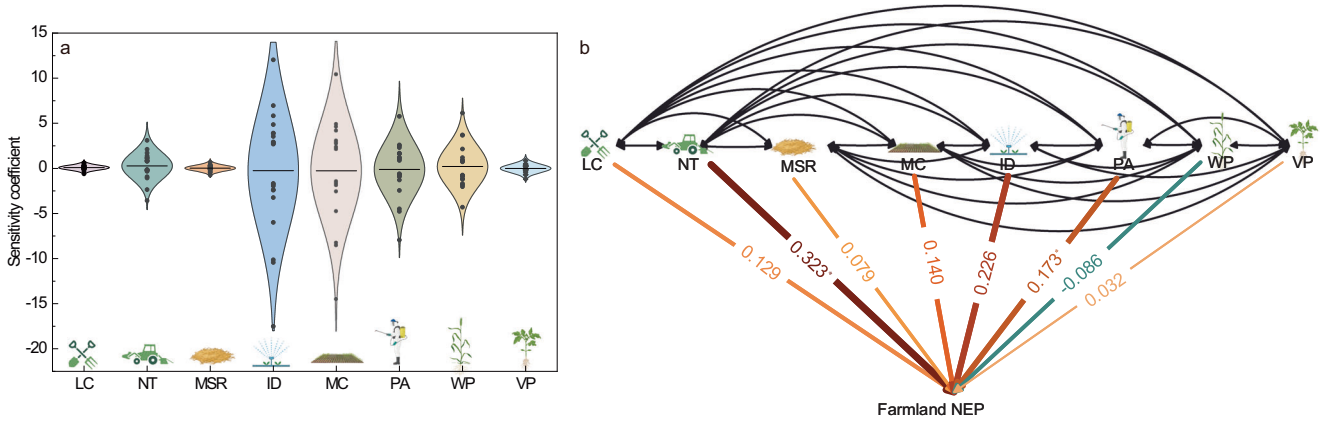

Fig. 4 | The response of farmland NEP to various human interventions from 2000 to 2020. A violin chart for sensitivity analysis of human interventions from 2000 to 2020 (**a**). NEP net ecosystem productivity, LC land consolidation, NT no-tillage, MSR mechanized straw returning, ID irrigation degree per unit area, MC multiple cropping level, PA pesticide amount per unit area, WP wheat planting proportion, VP vegetable planting proportion. The black dots in the figure represent the sensitivity coefficients of various human intervention activities each year. The horizontal line represents the annual average sensitivity coefficient. The protrusion on the violin chart represents extreme values. The temporal trend of sensitivity coefficients for each human intervention is shown in Supplementary Fig. 12. Path analysis diagram of farmland NEP changes (**b**). It describes the direct path coefficient (in color) and indirect path coefficient (in black) of variables on the farmland NEP. The thickness of the colored line represents the degree of influence. Specific indirect impacts of human interventions on farmland NEP from 2000 to 2020 can be found in Supplementary Table 1, and pathway analyses for different time periods can be found in Supplementary Tables 2 and 3. *, ** and *** indicate that the correlation coefficients pass through the significance levels of 10%, 5%, and 1%, respectively; and the *p*-values come from two-sided *t*-tests. Created in BioRender. Zhang, S. (2024) BioRender.com/z66f312.

(Supplementary Fig. 12), because, during this period, the farmland NEP shifts from a carbon source to a carbon sink. A graph of the temporal trend of the sensitivity coefficients for each human intervention activity, provided in the Supplementary information (Supplementary Fig. 12), shows that the response of farmland NEP to LC, NT and MC has gradually increased from 2000 to 2020[9,25]. Overall, LC ($R^2 = 0.395$) responds most strongly to farmland NEP.

We employed path analysis to further investigate the correlation coefficients and assess the relative significance of human interventions on the growth of farmland NEP from 2000 to 2020 ("Methods", Fig. 4b). Within the process of carbon sequestration in farmland, we found that MSR reduces the invasion of pests and diseases through the indirect effect of pesticide amount per unit area (PA), consequently enhancing the farmland NEP. By minimizing soil disturbance through NT practices and augmenting soil water demand via irrigation, the influence of LC on farmland NEP is indirectly intensified (Supplementary Table 1 and Fig. 4b). The dominant factors influencing farmland NEP changed from WP and MC in 2000 to LC and MSR in 2020 (Supplementary Table 4). LC and NT contribute significantly throughout the study period, indicating that they can increase carbon input and reduce carbon loss by reducing soil disturbance[9].

Subsequently, we performed a regression analysis to examine the relationship between major human interventions and farmland NEP. The results of the linear regression, as presented in Supplementary Table 5, indicate that the extent of five major human interventions positively affects farmland NEP, albeit to a lesser extent. This may imply the existence of a nonlinear relationship. Alternatively, there may also be measurement errors or omitted variables biases that confound the relationship. Then, using instrumental variables and introducing quadratic terms ("Methods"), we estimate the relationship between major human interventions and farmland NEP (Fig. 5 and Supplementary Table 6). The results reveal an inverted U-shaped relationship between LC and farmland NEP (inflection point of 2.62%), whereas NT and MSR exhibit a U-shaped relationship with farmland NEP (inflection point of 0.003% and 2.03%). Most regions are situated to the left of the LC inflection point and to the right of the NT and MSR inflection points (Supplementary Fig. 13), suggesting that farmland management practices are beneficial for carbon sequestration. LC directly impacts the soil by improving soil structure, optimizing water management, facilitating soil and root respiration, thereby enhancing carbon retention[42]. With increasing proportions of LC, the area under improvement in moderately and low-yielding fields expands, potentially leading to inefficient reclamation areas. Subsequent management issues following LC may also render some land difficult to utilize[43]. Therefore, transformed moderately and low-yielding fields exhibit limited carbon sequestration capacity, resulting in an inverted U-shaped relationship between LC and farmland NEP. Similarly, NT lowers soil temperature and decreases crop yields[15] and MSR results in residue coverage that hinders microbial growth[22]. At lower proportions of NT and MSR, there is no positive impact on carbon sequestration, and there may even be a negative impact. As the proportions of NT and MSR increase to achieve an ecological balance, soil organic carbon increases. Notably, prolonged increases can lead to soil compaction[44], a higher carbon-to-nitrogen ratio, and decreased straw decomposition rates[45], thereby causing a decline in soil carbon content.

The significant increase in farmland NEP in the MGPA is largely associated with LC (0.874, $p < 0.01$), NT (0.416, $p < 0.01$) and MC (0.364, $p < 0.01$) (Fig. 5b and Supplementary Table 6b). The MGSA contains a high proportion of non-grain farmland for the cultivation of cash crops such as vegetables, serving urban development. The combination of LC and cash crop cultivation in agricultural management ensures the stability of carbon sequestration. The increase in PSBA is related to irrigation degree per unit area (ID) (0.292, $p < 0.01$) and MC (0.385, $p < 0.01$) (Fig. 5d and Supplementary Table 6d). Specifically, irrigation has a negative effect on both the MGPA and the MGSA (−1.701, $p < 0.1$; −2.977, $p > 0.1$, in 2015–2020), while it has a positive effect on PSBA (3.439, $p > 0.1$, in 2015–2020) (Supplementary Table 7). The degree of irrigation in different regions leads to differences in soil moisture content and anaerobic conditions[12]. There are a number of different aspects that help to explain carbon sequestration in the PSBA: it is situated in western China, which, in comparison with the east, is less economically developed and has less annual precipitation (Supplementary Fig. 5). Compared to other regions, agricultural production in this area is notably more affected by hydrological conditions, particularly in the surface soils of arid and semi-arid zones, where

https://doi.org/10.1038/s41467-024-54907-6

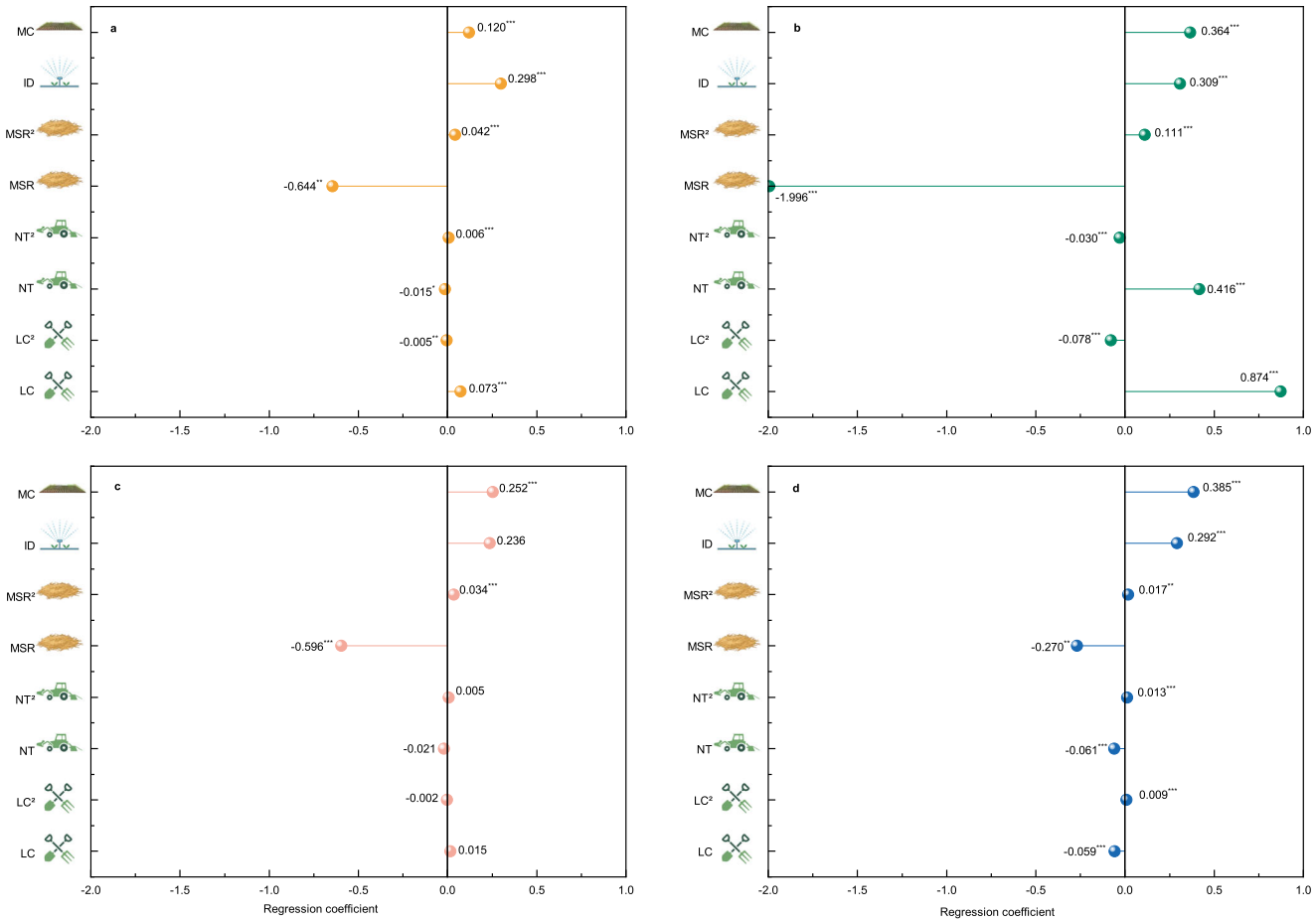

Fig. 5 | Regression analysis of major human interventions on farmland NEP based on instrumental variables. a, **b**, **c** and **d** are regression results for research areas, MGPA, MGSA and PSBA, respectively. NEP net ecosystem productivity, MGPA major grain-producing areas, MGSA major grain sales areas, PSBA production and sales balance areas, LC land consolidation, NT no-tillage, MSR mechanized straw returning, ID irrigation degree per unit area, MC multiple cropping level. LC^2, quadratic terms of land consolidation; NT^2, quadratic terms of no-tillage; MSR^2, quadratic terms of mechanized straw returning. *, **, *** denote significance at 10%, 5%, and 1%, respectively; and *p*-values from two-sided z-tests are listed under robust standard errors. The specific calculation details are given in "Methods". Created in BioRender. Zhang, S. (2024) BioRender.com/z66f312.

irrigation has a greater impact on plant growth than microbial decomposition[46]. Irrigation creates a favorable environment for microbial decomposition by regulating soil temperature, humidity and porosity, increasing organic matter input[47]. Additionally, the implementation of MSR is relatively slow in western China (with low adoption rates or short adoption durations), yet this phase of MSR still significantly enhances soil carbon sequestration. It enhances soil aggregation, increases organic matter content, fosters a conducive environment for microbial growth and reproduction, and facilitates microbial decomposition[45,48].

Our estimates of the relationship between farmland NEP and major human intervention activities are robust, as confirmed by several tests, including replacing the model (Supplementary Table 8a), substituting the dependent variable (Supplementary Table 8b–d), excluding certain regions (Supplementary Table 8e), and applying winsorization (Supplementary Table 8f). The specific analysis process can be found in the methods. The results show that the robustness results are consistent with the baseline results, validating the positive impact of major human interventions on farmland NEP.

Impacts of carbon cycle in the MGPA

To make progress in uncovering the relationship between major human interventions and farmland NEP, we investigate the relationship between the two in the MGPA. The proportion of farmland in the MGPA is large[49], and the changes in farmland NEP are more significant there than in the other areas (Fig. 1 and Supplementary Fig. 2). We have, therefore, focused on analyzing the carbon cycle process within the MGPA. In general, the continuous development and advancement of conservation tillage, such as NT and MSR, play a crucial role in soil and water conservation, reducing greenhouse gas emissions, and providing a significant opportunity for China's farmland to sequester atmospheric carbon[9,10,18]. First, NT reduces soil disturbance and promotes soil aggregation[9]. It has higher soil moisture levels and lower soil temperature than conventional tillage[50], which slows down the degradation rate of organic residues and reduces soil porosity and respiration, thereby slowing down carbon turnover and increasing soil carbon storage[9]. Second, straw can be directly used as a carbon source to increase carbon input through microbial decomposition, thereby directly increasing soil organic carbon content[51]. In addition, this practice can improve soil fertility and reduce the mineralization of soil organic carbon by microorganisms.

Since MSR and NT often act simultaneously on farmland[50], we considered whether their combined and individual effects on farmland NEP have changed (Supplementary Table 9). The value of −0.646 ($p < 0.01$) (Supplementary Table 9) indicates that NT + MSR still has a negative effect on farmland NEP. Since 2009, a large number of policies have emerged regarding MSR. After more than a decade of straw return, the increase in soil organic carbon content has slowed down,

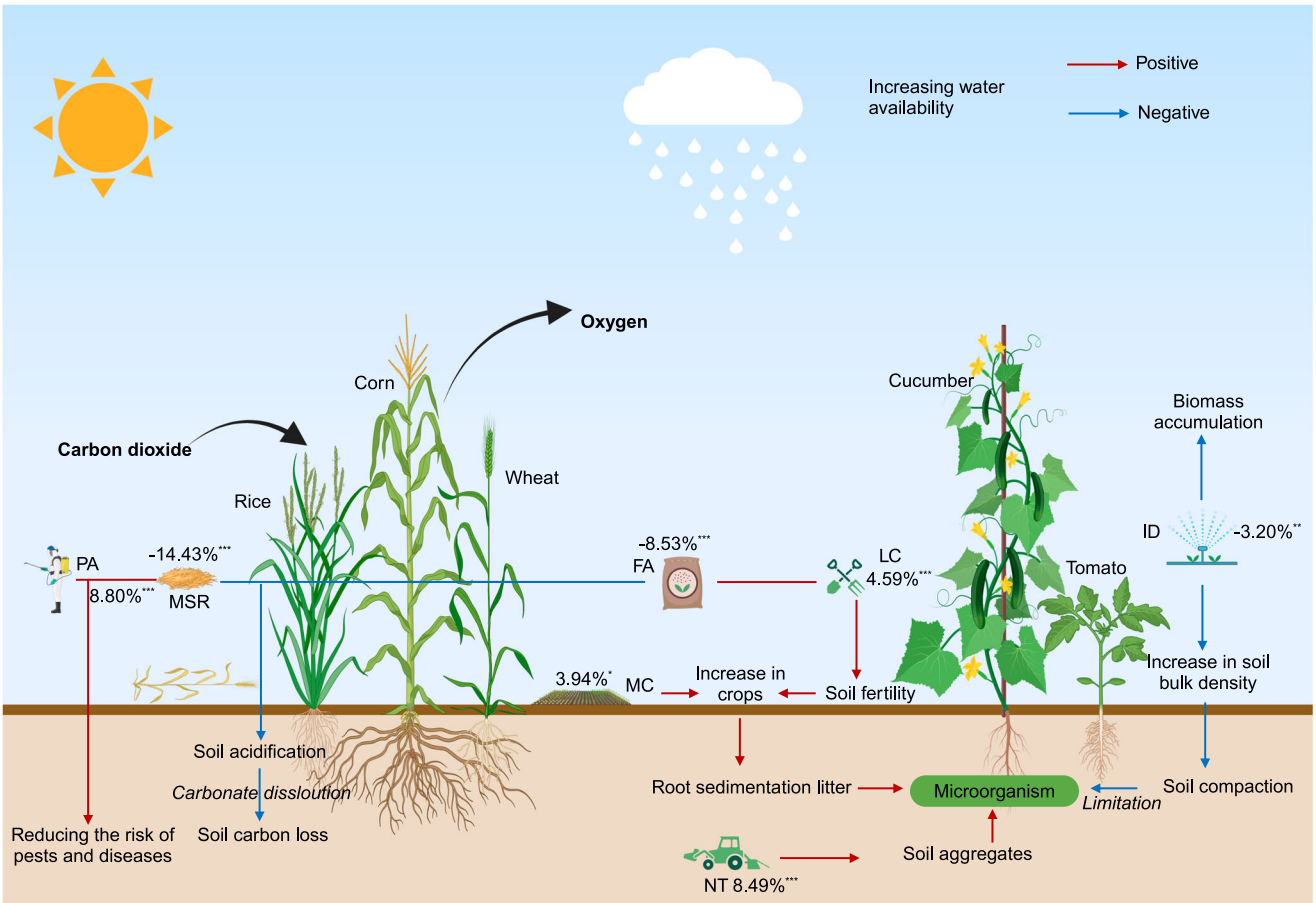

Fig. 6 | Mechanism and process of affecting carbon sequestration in farmland (MGPA in 2020). LC land consolidation, NT no-tillage, MSR mechanized straw returning, ID irrigation degree per unit area, MC multiple cropping level, PA pesticide amount per unit area, FA fertilization amount per unit area, MGPA major grain-producing areas. In 2020, the introduction of MC and LC introduces multicollinearity issues, so the coefficients of MC and LC were substituted with the computed results from all research areas in 2020. Figure created with Biorender.com. Created in BioRender. Zhang, S. (2024) BioRender.com/z66f312.

gradually reaching saturation[10,22]. Further increase in the MSR would lead to a higher carbon-to-nitrogen ratio, slowing down straw decomposition, and consequently impeding soil carbon sequestration[10,22,45]. Supplementary Table 10 shows the carbon sequestration situation in farmlands before and after the large-scale promotion of MSR. Under fertilization conditions, especially with the use of low-cost nitrogen fertilizers, the land under MSR can easily become acidified, leading to carbonate dissolution, subsequently causing a large reduction in soil carbon[37,52] (Fig. 6 and Supplementary Table 9). Additionally, MSR can cause pathogenic bacteria to return to the soil, exacerbating seeding and soil-borne diseases[37]. Farmland NEP has also been found to be affected by the interaction between MSR and PA (Supplementary Table 9), as reducing the risk of pests and diseases through PA enhances crop and carbon sequestration[53]. In a broader sense, MSR yields greater benefits than drawbacks. When conducted judiciously, it proves advantageous for both carbon sequestration and improved crop yields.

The carbon sequestration of farmland in the MGPA can be promoted through human intervention activities such as NT and LC (Fig. 6). Land consolidation increases the amount of available farmland through methods such as land leveling, thereby increasing crop yields and causing a 4.59% impact on carbon sequestration (in 2020). The MGPA contains a vast area of farmland, and the growth rate of farmland NEP is faster than in other regions. Additionally, this type of area is mainly used to grow wheat and corn, which have deeper and larger root systems compared to other grains such as rice, improving water uptake and enhancing soil carbon sequestration[35,36]. Humans have overcome the limitations of soil characteristics through measures such as ID and fertilization amount per unit area (FA)[54], thereby increasing the area of farmland and the soil carbon sequestration capacity. Fertilization promotes crop root production and increases crop yield, increasing soil organic carbon content[55]. The model results show that carbon sequestration in the MGPA, with its concentrated farmland, is positively affected by the factors.

Our results also show that irrigation has a slightly negative effect on carbon sequestration in farmland (Supplementary Table 7), which is contrary to the findings of other studies[20,46]. This discrepancy comes about because farmland irrigation in China's MGPA primarily relies on flood irrigation, which has a larger soil bulk density compared to drip irrigation[56]. Long-term excessive irrigation in certain areas has made the soil prone to compaction and lacking in granular structure: a condition which hampers root and microbial activity, leading to a decrease in carbon input and soil respiration[57]. Further, due to unstable hydrothermal conditions, it is also not conducive to the accumulation of underground biomass, resulting in poor carbon sequestration. Hence, irrigation in farmland should be kept at an optimal level, gradually transitioning from flood irrigation to more efficient drip irrigation. This shift can help reduce carbon emissions and enhance carbon sequestration.

Furthermore, we examined the carbon sequestration on farmland using the sample plots of the national field scientific observation and research stations as an example (Supplementary Tables 11 and 12).

Varietal replacement is also an important measure of human intervention in farmland. The distribution of varietal replacement at the national scale is too complex to be measured in detail. Through the analysis of yield changes demonstrated by varietal replacement, the results indicate that replacement in crop varieties within the sample plot has enhanced agricultural output, showing a positive correlation with the farmland NEP. Plants absorb carbon dioxide from the atmosphere during photosynthesis[58], and as the yield increases, there is, to a certain extent, a corresponding rise in carbon fixation to a certain extent. The results further suggest that MSR has a negative impact on carbon sequestration due to issues such as the resulting pests and diseases, as well as soil acidification (Supplementary Table 11—Taoyuan). Similarly, our examination of the relationship between fertilizers, pesticides, irrigation, and farmland NEP (Supplementary Table 12) revealed that carbon sequestration in farmlands is positively influenced by the use of fertilizers and pesticides. Switching from flood irrigation to furrow irrigation reduces the amount of irrigation water supplied, regulates soil water and salt conditions, and enhances root and microbial activity, thereby stimulating organic carbon sequestration in farmland[59]. In contrast, switching from sprinkler irrigation to furrow irrigation hinders carbon sequestration (Supplementary Table 12). Taken together, these results further confirm, from a micro perspective, the impact of human interventions on farmland NEP.

In summary, our work highlights the positive contribution of human interventions, especially LC, NT, and MC, to the ongoing transformation of farmland from carbon source to carbon sink (17.02%, MGPA in 2020). It emphasizes the fact that more attention should be paid to the positive role played by major human intervention activities, such as NT and LC, in farmland carbon sequestration. However, not all human interventions are positive. We find that the unreasonable practices of low MSR rates and extensive irrigation (Supplementary Note and Supplementary Figs. 12, 13), have a suppressive effect on farmland NEP (−17.63%, MGPA in 2020): a finding that differs from previous understanding. Effective carbon sequestration in farmland can be achieved through intensive rather than extensive irrigation practices (such as the adoption of drip irrigation) and the introduction of optimal MSR with moderate rates and quantities. Our research provides some new insights for analyzing the carbon sequestration of farmland ecosystems in other countries and reveals the significant, hidden role of human interventions driving farmland carbon sequestration. In agricultural production, better guidance on carbon sequestration can help alleviate the carbon emissions caused by climate change. Our work also has important implications for policy-makers attempting to develop sustainable and effective carbon sequestration strategies. High nature-value farmland, with a low intensity of farming and a high proportion of vegetation coverage, plays a crucial role in improving farmland carbon sequestration[60] and is the future development direction of farmland in China. A limitation of our study is that, due to the lack of detailed and small-scale statistical data, regional means were used in the process of combining statistical data with grid data. Future research should strive to quantify small-scale human agricultural activity data.

Methods

NEP dataset

Two NEP datasets from the National Earth System Science Data Center were used as benchmark dataset in this study. The first NEP dataset (NEP1) integrates flux observation network data, MODIS land products, GLASS data products, ERA5 meteorological data, and soil respiration data, covering the years 2000 to 2020 with a spatial resolution of 500 × 500 m[61]. The dataset's reliability is assessed through a five-fold independent cross-validation. The achieved R^2 value of 0.72 and root mean square error of 0.96 g C $m^{-2}day^{-1}$ indicate a reasonably robust model performance. The dataset employs a multi-faceted approach, combining observational data and techniques, and machine-learning methodologies to comprehensively analyze and model carbon exchange dynamics, accumulating monthly NEP values to obtain annual NEP data.

The second NEP dataset (NEP2) encompasses annual data on China's NPP and soil microbial respiration carbon emissions. This dataset spans from 2001 to 2021, with a spatial resolution of 1000 × 1000 m, sourced from Loess Plateau Science Data Center, National Earth System Science Data Sharing Infrastructure, National Science & Technology Infrastructure of China (http://loess.geodata.cn). As a crucial parameter in terrestrial ecological processes, NEP is calculated as the difference between NPP and soil microbial respiration carbon emissions. In this study, we compare the NEP1 dataset with the NEP2 dataset. The different calculation methods employed by these two datasets allow for a more accurate interpretation of the changes in China's NEP, thereby verifying the accuracy of our research findings.

Farmland dataset

We used two land-use/land-cover change datasets, namely the China land cover dataset (CLCD)[62] and the land use/cover change dataset (LUCC)[63]. The CLCD provides annual data on land cover in China at a spatial resolution of 30 × 30 m, which is acquired via remote sensing methods. The LUCC dataset, based on Landsat remote sensing imagery from the United States, is constructed through manual visual interpretation to create a multi-temporal thematic land use database with a spatial resolution of 30 × 30 m. It is sourced from the Resource and Environmental Science Data Registration and Publishing System. These datasets enable the determination of cultivated land distribution in China, and their combined use enhances the accuracy of our results.

Farmland NEP modeling methods

We combined the two NEP datasets with the two land-use/land-cover change datasets, resulting in four sets of farmland NEP data (NEPCLCD1, a combination of the CLCD and NEP1; NEPLUCC1, a combination of the LUCC and NEP1; NEPCLCD2, a combination of the CLCD and NEP2; NEPLUCC2, a combination of the LUCC and NEP2). These datasets are shown in Supplementary Figs. 3 and 8 and compared with other farmland NEP data (Supplementary Fig. 1g). NEPCLCD1 serves as our baseline calculation, while the other three datasets are used to verify the accuracy of the farmland NEP estimates. During the calculation process, we resampled the farmland data to derive a dataset with the same resolution as the NEP data. Subsequently, the resampled farmland data was overlaid onto the NEP datasets, allowing us to obtain the required farmland NEP.

Using the same method, we ultimately obtained the remaining three sets of farmland NEP data: the NEPLUCC1 (covering farmland NEP from 2000 to 2020, with a spatial resolution of 500 × 500 m), NEPCLCD2 and NEPLUCC2 (covering farmland NEP from 2001 to 2020, with a spatial resolution of 1000 × 1000 m). These four datasets all use processed NEP data. Although different farmland NEP datasets may exhibit distinct interannual variability, they are consistent in their increasing trends (Supplementary Fig. 1g). Finally, we obtained farmland NEP from 33 provincial-level administrative units in China, including Hong Kong and Taiwan, but Macau. This is because Macau has an area of only 32.8 km^2 and is predominantly focused on secondary and tertiary industries, with minimal agricultural activity and negligible farmland. Consequently, we excluded Macau from our analysis.

Climate dataset

We used precipitation (PRE) and temperature (TEM) data from the ERA5-Land dataset (https://cds.climate.copernicus.eu/), which has a spatial resolution of 0.1° × 0.1°. Monthly precipitation and temperature data were processed using raster calculation tools to obtain annual average precipitate on raster data and average temperature raster data

(Supplementary Fig. 5). These datasets were used to analyze the relationship between climate change and farmland NEP.

Socio-economic data

To investigate the relationship between human interventions and farmland NEP, we used socio-economic data from the China Rural Statistical Yearbook[64], China Agricultural Machinery Industry Yearbook[65], China Statistical Yearbook[66], and official websites of various province-level administrative units. These data were meticulously curated and refined to create a China-wide dataset with a spatial resolution of approximately 0.2° × 0.2°, covering various factors, including LC, NT, MSR, MC, ID, agricultural mechanization (AM) and crop planting structure from 2000 to 2020. These provide assurance for subsequent research and are crucial for assessing the impact of farmland NEP.

To conduct a more detailed micro-level analysis of farmland carbon sequestration, we selected sample plot data from the National Field Science Observation and Research Stations, accessed through the National Ecosystem Science Data Center, National Science & Technology Infrastructure of China (http://www.nesdc.org.cn; http://rs.cern.ac.cn). These data demonstrate the variation of crop varieties across various sample plots[67] (Supplementary Table 11), providing a more scientific and practical perspective for the analysis of fertilizers, pesticides, irrigation, and other aspects of farmland ecosystems at Changshu[68,69], Fengqiu[70,71], Changwu[72,73], Luancheng[74,75], Shenyang[76,77], and Taoyuan stations[78,79] (Supplementary Table 12). This micro-level analysis complements the macro-level research and strongly supports the findings of this study.

Spatial characteristics analysis

First, to assess the trend in farmland NEP changes from 2000 to 2020, we adopted a unary linear regression analysis. This approach is widely used in trend analysis and allows us to calculate the trend slopes of multi-year regressions at the pixel level. These slopes represent the interannual rate of changes in farmland NEP. The positive or negative sign of the trend rate indicates an increasing or decreasing trend, respectively, while the magnitude reflects the rate of this change (Fig. 2a). Significant and non-significant change areas were identified through significance testing (F-test) (Fig. 1b). This provides insight into how carbon sequestration on farmland has evolved over the study period.

$$\theta_{Slope} = \frac{n \times \sum_{i=1}^{n}(i \times X_i) - \left(\sum_{i=1}^{n} i\right) \times \left(\sum_{i=1}^{n} X_i\right)}{n \times \sum_{i=1}^{n} i^2 - \left(\sum_{i=1}^{n} i\right)^2} \quad (1)$$

where n represents the length of the time series being studied, i denotes the i-th year, X_i represents the farmland NEP in the i-th year, and θ_{Slope} represents the trend rate, indicating the rate at which the index changes over time.

Second, the stability of farmland NEP from 2000 to 2020 was determined by the standard deviation, which reflected the degree of dispersion of the data fluctuations. The larger the standard deviation, the greater the interannual variation and the instability of farmland NEP during the study period. We applied the Natural Breaks (Jenks) method to categorize stability into higher stability, high stability, moderate stability, low stability, and lower stability (Fig. 2b).

$$SD = \sqrt{\frac{\sum_{i=1}^{n}(NEP_i - \overline{NEP})^2}{n-1}} \quad (2)$$

where SD is the standard deviation, $\overline{NEP}$ represents the n-year average of farmland NEP.

Third, due to the different values of farmland NEP between regions during different periods, the concept of relative development rate (Nich) was adopted to measure the difference in development speed. This is an indicator reflecting relative growth and can be used to analyze the relationship between changes of farmland NEP within different pixels and the overall changes. A Nich value greater than 1 signifies that the growth rate of farmland NEP within the grid exceeds the overall development rate, while a value less than 1 indicates a growth rate lower than the overall development rate (Fig. 2c).

$$Nich = \frac{NEP_{starting-a} - NEP_{ending-a}}{\overline{NEP_{starting}} - \overline{NEP_{ending}}} \quad (3)$$

where $Nich$ is the relative development rate, $NEP_{starting\text{-}a}$ and $NEP_{ending\text{-}a}$ represent the NEP values of farmland in the starting and ending years within the a-th grid, respectively. $\overline{NEP_{starting}}$ and $\overline{NEP_{ending}}$ are the average of farmland NEP in the starting and ending years.

Fourth, the model of the shifting center of gravity reveals changes in the spatial evolution of a variable, highlighting the changing trends and spatial characteristics of farmland NEP within the region. We used it here to reflect the transfer direction of the center of gravity of farmland NEP from 2000 to 2020 (Fig. 1c, d and Supplementary Fig. 8).

$$X = \frac{\sum_{a=1}^{A}(NEP_a \times x_a)}{\sum_{a=1}^{A} NEP_a}$$
$$Y = \frac{\sum_{a=1}^{A}(NEP_a \times y_a)}{\sum_{a=1}^{A} NEP_a} \quad (4)$$
$$D_{j-i} = R \times \sqrt{(Y_j - Y_i)^2 + (X_j - X_i)^2}$$

where X and Y are the longitude and latitude of the gravity center, respectively, NEP_a is the farmland NEP in the a-th grid. x_a and y_a are the longitude and latitude of the a-th grid, respectively. $D_{j\text{-}i}$ represents the distance of the gravity center shift between two different years, where i and j denote these years. The coordinates (X_i, Y_i) and (X_j, Y_j) represent the geographical positions of the gravity center in the i-th and j-th years, respectively. R is a constant, set at 111.111 km.

Statistical analysis

Path analysis. We conducted path analysis to better understand the direct and indirect effects of human interventions on farmland NEP and reflect their surface correlations. In explaining human interventions, we selected various variables related to activities such as farmland management. We established linear regression equations to obtain the correlation between various human interventions and farmland NEP. Additionally, we divided the study period into two segments (the first 11 years and the subsequent 10 years) to capture their relationships more precisely. On this basis, the direct path coefficient, the indirect path coefficient and the residual effect can be calculated, enabling a path map to be drawn (Fig. 4b). P-values from two-sided t-tests are listed under standard errors.

Sensitivity analysis. The relationship between farmland NEP and human interventions is becoming increasingly close. To quantitatively describe the response of various human interventions to changes in farmland NEP, we adopted a sensitivity coefficient method based on the partial derivative principle. The sensitivity coefficient is the ratio of the change rate of farmland NEP to the change rate of various human interventions. We then calculated the relative contribution rates of each factor, based on the relative rates of change and sensitivity coefficient of the factors.

Pearson correlation analysis. We used the Pearson correlation coefficient to calculate the correlation between farmland NEP and the various influencing factors. We focused on the correlation coefficient of the areas with concentrated farmland distribution (such as the North China Plain and the Northeast Plain). For the climate factors, we combined data with a resolution of 0.1° × 0.1° and farmland NEP to

generate two separate Pearson R maps (Supplementary Fig. 11a, b). For the human intervention factors, 13 Pearson correlation maps (Fig. 3 and Supplementary Fig. 11c–j) were generated at a resolution of 0.2° × 0.2°.

Multiple regression analysis. The response of farmland NEP changes is a complex system of multiple factors that are jointly affected by climate factors and human interventions. We used multiple regression analysis to explore the importance of each in the changes in farmland NEP. We merge human interventions, climate and farmland NEP data together to form a dataset. Due to the varying annual distribution ranges of farmland NEP, this dataset is an unbalanced panel dataset. This sample was used for all statistical analyses shown in Figs. 3–6, except as noted in the legends. Figure 3 illustrates the correlation between major human interventions and farmland NEP in China. Figure 4 presents sensitivity analysis and path analysis of human interventions and farmland NEP. Figure 5 includes regression analysis with quadratic terms to account for nonlinear relationships. Figure 6 depicts the mechanism between major human interventions and farmland NEP in 2020 in the MGPA.

Statistical analyses relating farmland NEP to human interventions are complicated by the fact that human interventions are correlated with many unobservable anthropogenic factors. These unobserved variables may induce spurious correlations between human interventions and farmland NEP, or bias regression coefficients towards zero, potentially leading to erroneous rejection of the null hypothesis. To overcome this challenge, we employed an instrumental variables approach. This method leverages a variable known as an "instrument" that does not directly affect farmland NEP but influences human interventions. In certain scenarios, this instrumental variable can be used in a 2SLS regression to isolate the variation in regression variables unrelated to the outcome, thereby improving the unbiased estimation of the variables of interest[80]. When estimating the major human interventions -farmland NEP, we specifically used DEM (Digital Elevation Model) data as an instrumental variable. Additionally, considering temporal factors and the fact that DEM is cross-sectional data, we lagged LC, NT, MSR, ID, and MC by one period and combined them with DEM to form respective instrumental variables. DEM does not directly affect farmland NEP and must act through other variables. This leads to significant changes in major human interventions (with coefficients in the first stage of 2SLS regression being significant at $p < 0.01$), making these instrumental variables effective for major human interventions. Accounting for spatial heterogeneity, we conducted regression estimates for the MGPA, MGSA, and PSBA regions respectively.

Before performing the regression analysis, we conducted a multicollinearity test to ensure that there is no significant correlation among the variables, and also conducted Hausman test to select fixed effects method. We implemented the instrumental variables through 2SLS, which includes the following two equations.

$$MHI_{iab} = \varphi IV_{iab} + \chi M_{ia} + \alpha_i + \varepsilon_{iab} \quad (5)$$

$$NEP_{iab} = \beta MHI'_{iab} + \gamma M_{ia} + \alpha_i + \mu_{iab} \quad (6)$$

where i indicates year and a indicates raster. IV_{iab} is the instrumental variables for the explanatory variable b in the i-th year of the a-th raster. MHI_{iab} is the b-th major human interventions for the i-th year and a-th raster, mainly including LC, NT, MSR, ID, and MC. Equation (5) estimates the relationship between major human interventions and instrumental variables, while Eq. (6) uses predicted values from Eq. (5) in place of the observed major human interventions to estimate the relationship between farmland NEP and major human interventions. M_{ia} is the control variable, such as TEM, PRE, FA, PA, AM, WP, rice planting proportion (RP), corn planting proportion (CP), oil planting proportion (OP), and VP. The terms ε_{iab} and μ_{iab} indicate model error terms, and in both equations, standard errors are clustered at the raster level. α_i indicates a set of dummy variables for each raster, and these spatial "fixed effects" account for all time-invariant characteristics of each raster. Due to the potential significant spatial variation in the instrumental variable (DEM), these spatial fixed effects ensure that our interpretation of the dependent variable excludes comparisons between different locations.

Simultaneously, we did not consider time fixed effects, as our primary focus is on the impact of human interventions on farmland NEP rather than the differences across various years. The number of time periods is relatively small compared to the number of cross-sections. Additionally, the time effects have already been captured by the explanatory variables (LC, NT, MSR, ID, etc.), rendering the inclusion of time effects redundant. Furthermore, the introduction of time effects resulted in multicollinearity, leading to the omission of several years. Adding time fixed effects did not significantly enhance the model's explanatory power. Therefore, we opted against including time fixed effects to preserve the model's simplicity and explanatory capability. After adjusting for spatial variations through individual fixed effects method, we obtained relatively robust results. The testing of instrumental variables can be found in Supplementary Tables 6–8 and 10.

To strengthen the validity of causal relationships and bolster the credibility of our model, we conducted a series of robustness tests. First, we replaced the 2SLS method with the GMM model to recalculate the results (Supplementary Table 8a). Second, by substituting the dependent variable, we verified the robustness of the model results using the other three sets of farmland NEP data (Supplementary Table 8b–d). Third, the urban planning of Chinese municipalities directly under the central government differs from that of other regions, leading to discrepancies in farmland management. Similarly, Tibet, Qinghai, and Hainan have relatively small areas dedicated to agricultural cultivation. Therefore, we proposed excluding these seven regions to ensure the robustness of the test results (Supplementary Table 8e). Additionally, in the estimations, to reduce the impact of extreme values, farmland NEP was winsorized at the 1% level (Supplementary Table 8f). These robustness tests significantly bolster the reliability of our model for publication.

Data availability

All data enabling our analysis are openly available, and their sources are detailed in "Methods" and Supplementary Information. The NEP datasets used in this study are available at https://www.geodata.cn/ and http://loess.geodata.cn. The farmland datasets are available at http://irsip.whu.edu.cn/ and https://www.resdc.cn/. The climate data of the ERA5-Land dataset is available at https://cds.climate.copernicus.eu/. The sample plot data from the National Field Science Observation and Research Stations are available at http://www.nesdc.org.cn and http://rs.cern.ac.cn. The datasets used to generate all the figures in the article and its Supplementary Information are publicly available at Figshare (https://doi.org/10.6084/m9.figshare.27841734.v1).

References

1. Gampe, D. et al. Increasing impact of warm droughts on northern ecosystem productivity over recent decades. *Nat. Clim. Change* **11**, 772–779 (2021).
2. Friedlingstein, P. et al. Global carbon budget 2023. *Earth Syst. Sci. Data.* **15**, 5301–5369 (2023).
3. Chen, J. et al. Vegetation structural change since 1981 significantly enhanced the terrestrial carbon sink. *Nat. Commun.* **10**, 4259 (2019).

4. Ballantyne, A. P., Alden, C. B., Miller, J. B., Tans, P. P. & White, J. W. C. Increase in observed net carbon dioxide uptake by land and oceans during the past 50 years. *Nature* **488**, 70–72 (2012).
5. Food and Agriculture Organization of the United Nations. *Land Use*. FAOSTAT. https://www.fao.org/faostat/en/#data/RL (2020).
6. Ellis, E. C. & Ramankutty, N. Putting people in the map: anthropogenic biomes of the world. *Front. Ecol. Environ.* **6**, 439–447 (2008).
7. Searchinger, T. D., Wirsenius, S., Beringer, T. & Dumas, P. Assessing the efficiency of changes in land use for mitigating climate change. *Nature* **564**, 249–253 (2018).
8. Medková, H., Vačkář, D. & Weinzettel, J. Appropriation of potential net primary production by cropland in terrestrial ecoregions. *J. Clean. Prod.* **150**, 294–300 (2017).
9. Lu, F. et al. Soil carbon sequestrations by nitrogen fertilizer application, straw return and no-tillage in China's cropland. *Glob. Change Biol.* **15**, 281–305 (2009).
10. Liu, C., Lu, M., Cui, J., Li, B. & Fang, C. Effects of straw carbon input on carbon dynamics in agricultural soils: a meta-analysis. *Glob. Change Biol.* **20**, 1366–1381 (2014).
11. Berhane, M. et al. Effects of long-term straw return on soil organic carbon storage and sequestration rate in North China upland crops: a meta-analysis. *Glob. Change Biol.* **26**, 2686–2701 (2020).
12. Shang, Z. et al. Can cropland management practices lower net greenhouse emissions without compromising yield? *Glob. Change Biol.* **27**, 4657–4670 (2021).
13. Bastos, A. et al. Direct and seasonal legacy effects of the 2018 heat wave and drought on European ecosystem productivity. *Sci. Adv.* **6**, eaba2724 (2020).
14. Ritchie, P. D. L. et al. Shifts in national land use and food production in Great Britain after a climate tipping point. *Nat. Food* **1**, 76–83 (2020).
15. Pittelkow, C. M. et al. Productivity limits and potentials of the principles of conservation agriculture. *Nature* **517**, 365–368 (2015).
16. Ciais, P. et al. Europe-wide reduction in primary productivity caused by the heat and drought in 2003. *Nature* **437**, 529–533 (2005).
17. Kim, J. et al. Reduced North American terrestrial primary productivity linked to anomalous Arctic warming. *Nat. Geosci.* **10**, 572–576 (2017).
18. Lal, R. Soil carbon sequestration impacts on global climate change and food security. *Science* **304**, 1623–1627 (2004).
19. Lal, R. Residue management, conservation tillage and soil restoration for mitigating greenhouse effect by CO_2-enrichment. *Soil. Res.* **43**, 81–107 (1997).
20. Follett, R. F. Soil management concepts and carbon sequestration in cropland soils. *Soil Res.* **61**, 77–92 (2001).
21. Wang, H. et al. Tillage system change affects soil organic carbon storage and benefits land restoration on loess soil in North China. *Land Degrad. Dev.* **29**, 2880–2887 (2018).
22. Wang, Y. et al. Does continuous straw returning keep China farmland soil organic carbon continued increase? A meta-analysis. *J. Environ. Manag.* **288**, 112391 (2021).
23. Freibauer, A., Rounsevell, M. D. A., Smith, P. & Verhagen, J. Carbon sequestration in the agricultural soils of Europe. *Geoderma* **122**, 1–23 (2004).
24. Prairie, A. M., King, A. E. & Cotrufo, M. F. Restoring particulate and mineral-associated organic carbon through regenerative agriculture. *Proc. Natl Acad. Sci. USA* **120**, e2217481120 (2023).
25. Yang, X. et al. Diversifying crop rotation increases food production, reduces net greenhouse gas emissions and improves soil health. *Nat. Commun.* **15**, 198 (2024).
26. Zhai, Y. et al. Can grain virtual water flow reduce environmental impacts? Evidence from China. *J. Clean. Prod.* **314**, 127970 (2021).
27. Nation Development and Reform Commission. *Outline of the National Medium- and Long-Term Plan for Food Security (2008–2020)*. https://www.ndrc.gov.cn/ (2008).
28. Zhang, L., Pang, J., Chen, X. & Lu, Z. Carbon emissions, energy consumption and economic growth: evidence from the agricultural sector of China's main grain-producing areas. *Sci. Total Environ.* **665**, 1017–1025 (2019).
29. Guo, J. et al. Significant acidification in major Chinese croplands. *Science* **327**, 1008–1010 (2010).
30. Bi, X., Pan, X. & Zhou, S. Soil security is alarming in China's main grain producing areas. *Environ. Sci. Technol.* **47**, 7593–7594 (2013).
31. Wei, D. et al. Elevation-dependent pattern of net CO_2 uptake across China. *Nat. Commun.* **15**, 2489 (2024).
32. Keenan, T. F. et al. Recent pause in the growth rate of atmospheric CO_2 due to enhanced terrestrial carbon uptake. *Nat. Commun.* **7**, 13428 (2016).
33. Zhao, M. & Running, S. W. Drought-induced reduction in global terrestrial net primary production from 2000 through 2009. *Science* **329**, 940–943 (2010).
34. He, H. et al. Altered trends in carbon uptake in China's terrestrial ecosystems under the enhanced summer monsoon and warming hiatus. *Natl Sci. Rev.* **6**, 505–514 (2019).
35. Lynch, J. P. & Wojciechowski, T. Opportunities and challenges in the subsoil: pathways to deeper rooted crops. *J. Exp. Bot.* **66**, 2199–2210 (2015).
36. Yamauchi, A., Kono, Y. & Tatsumi, J. Comparison of root system structures of 13 species of cereals. *Jpn. J. Crop Sci.* **56**, 678–631 (1987).
37. Zhao, Y. et al. Economics- and policy-driven organic carbon input enhancement dominates soil organic carbon accumulation in Chinese croplands. *Proc. Natl Acad. Sci. USA* **115**, 4045–4050 (2018).
38. Ahlström, A. et al. The dominant role of semi-arid ecosystems in the trend and variability of the land CO_2 sink. *Science* **348**, 895–899 (2015).
39. Piao, S. et al. The carbon balance of terrestrial ecosystems in China. *Nature* **458**, 1009–1013 (2009).
40. Xin, F. et al. Large increases of paddy rice area, gross primary production, and grain production in Northeast China during 2000–2017. *Sci. Total Environ.* **711**, 135183 (2020).
41. Ran, Y. et al. Distribution of permafrost in China: an overview of existing permafrost maps. *Permafr. Periglac.* **23**, 322–333 (2012).
42. Chen, X. et al. The impact of land consolidation on arable land productivity: a differentiated view of soil and vegetation productivity. *Agr. Ecosyst. Environ.* **326**, 107781 (2022).
43. Du, X., Zhang, X. & Jin, X. Assessing the effectiveness of land consolidation for improving agricultural productivity in China. *Land Use Policy* **70**, 360–367 (2018).
44. Nunes, M. R., Denardin, J. E., Pauletto, E. A., Faganello, A. & Pinto, L. F. S. Mitigation of clayey soil compaction managed under no-tillage. *Soil. Res.* **148**, 119–126 (2015).
45. Jin, Z. et al. Effect of straw returning on soil organic carbon in rice–wheat rotation system: a review. *Food Energy Secur.* **9**, e200 (2020).
46. Emde, D., Hannam, K. D., Most, I., Nelson, L. M. & Jones, M. D. Soil organic carbon in irrigated agricultural systems: a meta-analysis. *Glob. Change Biol.* **27**, 3898–3910 (2021).
47. Denef, K., Stewart, C. E., Brenner, J. & Paustian, K. Does long-term center-pivot irrigation increase soil carbon stocks in semi-arid agro-ecosystems? *Geoderma* **145**, 121–129 (2008).
48. Lou, Y. et al. Straw coverage alleviates seasonal variability of the topsoil microbial biomass and activity. *CATENA* **86**, 117–120 (2011).
49. Kong, L. et al. Natural capital investments in China undermined by reclamation for cropland. *Nat. Ecol. Evol.* **7**, 1771–1777 (2023).

50. Guo, L. et al. Effects of long-term no tillage and straw return on greenhouse gas emissions and crop yields from a rice-wheat system in central China. *Agr. Ecosyst. Environ.* **322**, 107650 (2021).
51. Islam, M. U., Jiang, F., Guo, Z., Liu, S. & Peng, X. Impacts of straw return coupled with tillage practices on soil organic carbon stock in upland wheat and maize croplands in China: a meta-analysis. *Soil. Res.* **232**, 105786 (2023).
52. Raza, S. et al. Dramatic loss of inorganic carbon by nitrogen-induced soil acidification in Chinese croplands. *Glob. Change Biol.* **26**, 3738–3751 (2020).
53. Tilman, D. et al. Forecasting agriculturally driven global environmental change. *Science* **292**, 281–284 (2001).
54. Ramankutty, N., Foley, J. A., Norman, J. & McSweeney, K. The global distribution of cultivable lands: current patterns and sensitivity to possible climate change. *Glob. Ecol. Biogeogr.* **11**, 377–392 (2002).
55. Hutchinson, J. J., Campbell, C. A. & Desjardins, R. L. Some perspectives on carbon sequestration in agriculture. *Agr. For. Meteorol.* **142**, 288–302 (2007).
56. Hondebrink, M. A., Cammeraat, L. H. & Cerdà, A. The impact of agricultural management on selected soil properties in citrus orchards in Eastern Spain: a comparison between conventional and organic citrus orchards with drip and flood irrigation. *Sci. Total Environ.* **581–582**, 153–160 (2017).
57. Mudge, P. L. et al. Irrigating grazed pasture decreases soil carbon and nitrogen stocks. *Glob. Change Biol.* **23**, 945–954 (2017).
58. Piao, S. et al. Net carbon dioxide losses of northern ecosystems in response to autumn warming. *Nature* **451**, 49–52 (2008).
59. Ball, K. R., Malik, A. A., Muscarella, C. & Blankinship, J. C. Irrigation alters biogeochemical processes to increase both inorganic and organic carbon in arid-calcic cropland soils. *Soil Biol. Biochem.* **187**, 109189 (2023).
60. Boyle, P., Hayes, M., Gormally, M., Sullivan, C. & Moran, J. Development of a nature value index for pastoral farmland—a rapid farm-level assessment. *Ecol. Indic.* **56**, 31–40 (2015).
61. Huang, N., Wang, L., Zhang, Y., Gao, S. & Niu, Z. Estimating the net ecosystem exchange at global FLUXNET sites using a random forest model. *IEEE J.-SRARS* **14**, 9826–9836 (2021).
62. Yang, J. & Huang, X. The 30 m annual land cover dataset and its dynamics in China from 1990 to 2019. *Earth Syst. Sci. Data* **13**, 3907–3925 (2021).
63. Xu, X. et al. *Multi-period Land Use Remote Sensing Monitoring Dataset in China (CNLUCC)*. Resource and Environmental Science Data Registration and Publishing System. http://www.resdc.cn/DOI, https://doi.org/10.12078/2018070201 (2018).
64. CRSY. *China Rural Statistical Yearbook* (China Statistics Press, 2001–2021).
65. CAMIY. *China Agricultural Machinery Industry Yearbook* (Machinery Industry Press, 2001–2021).
66. CSY. *China Statistical Yearbook* (China Statistics Press, 2001–2021).
67. National Ecosystem Observation and Research Network/China Ecosystem Research Network. *National Ecosystem Observation and Research Network Technology Resource Service System*. http://www.cnern.org.cn (2015).
68. Jiangsu Changshu Station. *Monitoring Data of Farming Systems at Changshu Station, Jiangsu Province (1999–2006)*. National Ecological Science Data Center. https://doi.org/10.12199/nesdc.ecodb.mon.2020.dp2011.csa.002 (2021).
69. Yan, X., Liu, Q. & Lin, J. *Chinese Ecosystem Positioning Observation and Research Dataset: Farmland Ecosystem Volume—Changshu Station, Jiangsu (1998–2006)* (China Agriculture Press, 2010).
70. Henan Fengqiu Station. *Monitoring Data of Crop Harvest Period at Fengqiu Station, Henan Province (2004–2008)*. National Ecological Science Data Center. https://doi.org/10.12199/nesdc.ecodb.mon.2020.dp2011.csa.002 (2020).
71. Zhang, J., Wang, J. & Xin, X. *Chinese Ecosystem Positioning Observation and Research Dataset: Farmland Ecosystem Volume—Fengqiu Station, Henan (1998–2008)* (China Agriculture Press, 2010).
72. Shaanxi Changwu Station. *Monitoring Data of Farmland Planting Management at Changwu Station, Shaanxi Province (1998–2008)*. National Ecological Science Data Center. https://doi.org/10.12199/nesdc.ecodb.mon.2020.dp2011.cwa.001 (2020).
73. Liu, W. & Dang, T. *Chinese Ecosystem Positioning Observation and Research Dataset: Farmland Ecosystem Volume—Changwu Station, Shaanxi (1998–2008)* (China Agriculture Press, 2012).
74. Hebei Luancheng Station. *Monitoring Data of Farmland Planting Management at Luancheng Station, Hebei Province (2001–2008)*. National Ecological Science Data Center. https://doi.org/10.12199/nesdc.ecodb.mon.2020.dp2011.lca.001 (2020).
75. Hu, C. & Cheng, Y. *Chinese Ecosystem Positioning Observation and Research Dataset: Farmland Ecosystem Volume—Luancheng Station, Hebei (1998–2008)* (China Agriculture Press, 2011).
76. Liaoning Shenyang Station. *Monitoring Data of Farming System at Shenyang Station, Liaoning Province (1998–2008)*. National Ecological Science Data Center. https://doi.org/10.12199/nesdc.ecodb.mon.2020.dp2011.sya.002 (2021).
77. Zheng, L. & Zhang, X. *Chinese Ecosystem Positioning Observation and Research Dataset: Farmland Ecosystem Volume—Shenyang Station, Liaoning (1998–2008)* (China Agriculture Press, 2010).
78. Chen, C. et al. *Dataset on Rice Root Biomass and Nutrient Content of Rice Root Observed by Taoyuan Agro-ecosystem Research Station, Chinese Academy of Sciences, 2005–2018*. National Ecological Science Data Center. https://doi.org/10.57760/sciencedb.08617 (2023).
79. Chen, C. et al. Dataset on rice root biomass and nutrient content of rice root observed by Taoyuan Agro-ecosystem Research Station, Chinese Academy of Sciences, 2005–2018. *Chin. Sci. Data* **8**, 226–237 (2023).
80. Zhang, P., Carleton, T., Lin, L. & Zhou, M. Estimating the role of air quality improvements in the decline of suicide rates in China. *Nat. Sustain.* **7**, 260–269 (2024).

Acknowledgements

W.C. was funded by the National Natural Science Foundation of China (grant no. 72074181) and the Major Project of the National Social Science Foundation of China (grant no. 22&ZD113). Y.W. was funded by the National Natural Science Foundation of China (grant no. 42401374). Z.S. was supported by the National Natural Science Foundation of China (grant no. 52200222), the Key Project of Philosophy and Social Sciences of China's Ministry of Education (grant no. 22JZD019), and Chinese Universities Scientific Fund (grant no. 2023TC098). We thank the National Ecosystem Observation and Research Network/Chinese Ecosystem Research Network Science and Technology Resource Service Platform (http://rs.cern.ac.cn), and National Ecosystem Science Data Center, National Science & Technology Infrastructure of China (http://www.nesdc.org.cn) for providing data support, with special thanks to the CSA Ecological Station, FQA Ecological Station, CWA Ecological Station, LCA Ecological Station, TYA Ecological Station, YCA Ecological Station, and YTA Ecological Station. We acknowledge the data support from "National Earth System Science Data Center, National Science & Technology Infrastructure of China (https://www.geodata.cn)," and "Loess Plateau Science Data Center, National Earth System Science Data Sharing Infrastructure, National Science & Technology Infrastructure of China (http://loess.geodata.cn)."

Author contributions

S.Z. and W.C. designed the research; S.Z. performed analysis and drafted the paper. W.C., Y.W. and Z.S. contributed to the supervision and

project administration. Q.L., H.S., M.L., B.Z. and G.S. contributed to data analysis and interpretation.

Competing interests
The authors declare no competing interests.

Additional information
Supplementary information The online version contains supplementary material available at https://doi.org/10.1038/s41467-024-54907-6.

Correspondence and requests for materials should be addressed to Wei Chen or Yanan Wang.

Peer review information *Nature Communications* thanks Chaoqing Huang and the other anonymous reviewer(s) for their contribution to the peer review of this work. A peer review file is available.